Histol Histopathol (2008) 23: 1353-1366

http://www.hh.um.es

Histology and Histopathology

Cellular and Molecular Biology

Vitamin k2, a γ-carboxylating factor of gla-proteins, normalizes the bone crystal nucleation impaired by Mg-insufficiency

Norio Amizuka[1], Minqi Li[1], Masatoshi Kobayashi[3], Kuniko Hara[3], Shoji Akahane[4], Kiichi Takeuchi[2], Paulo H.L. Freitas[2], Hidehiro Ozawa[4], Takeyasu Maeda[1,2] and Yasuhiro Akiyama[3]

[1]Center for Transdisciplinary Research, Niigata University, Niigata, Japan, [2]Division of Oral Anatomy, Niigata University Graduate School of Medical and Dental Sciences, Niigata, Japan, [3]Pharmacological Evaluation Section, Eisai Co., Ltd., Tokyo, Japan and [4]Institute for Oral Science, Matsumoto Dental University, Shiojiri, Japan

Summary. It has been reported that the Mg-insufficient bone is fragile upon mechanical loading, despite its high bone mineral density, while vitamin K2 (MK-4: menatetrenone) improved the mechanical strength of Mg-insufficient bone. Therefore, we aimed to elucidate the ultrastructural properties of bone in rats with dietary Mg insufficiency with and without MK-4 supplementation. Morphological examinations including histochemistry, transmission electron microscopy, electron probe microanalysis (EPMA) and X-ray diffraction were conducted on the femora and tibiae of 4-week-old Wistar male rats fed with 1) a normal diet (control group, 0.09% Mg), 2) a Mg-insufficient diet (low Mg group, 0.006% Mg), or 3) a Mg-insufficient diet supplemented with MK-4 (MK-4 group, 0.006% Mg, 0.03% MK-4). MK-4 appeared to inhibit the osteoclastic bone resorption that is stimulated by Mg insufficiency. EPMA analysis, however, revealed an increased concentration of Ca paralleling Mg reduction in the low Mg group. Assessment by X-ray diffraction revealed an abundance of a particular synthetic form of hydroxyapatite in the low Mg group, while control bones featured a variety of mineralized crystals. In addition, Mg-deficient bones featured larger mineral crystals, *i.e.*, crystal overgrowth. This crystalline aberration in Mg-insufficient bones induced collagen fibrils to mineralize easily, even in the absence of mineralized nodules, which therefore led to an early collapse of the fibrils. MK-4 prevented premature collagen mineralization by normalizing the association of collagen fibrils with mineralized nodules. Thus, MK-4 appears to rescue the impaired collagen mineralization caused by Mg insufficiency by promoting a re-association of the process of collagen mineralization with mineralized nodules.

Key words: Bone Mineralization, Magnesium, Vitamin K2 (menatetrenone), Hydroxyapatite

Offprint requests to: Norio Amizuka, DDS, PhD, Center for Transdisciplinary Research, Niigata University, 2-5274 Gakkocho-dori, Niigata 951-8514, Japan. e-mail: amizuka@dent.niigata-u.ac.jp

Introduction

Clinico-epidemiological studies have demonstrated a significant correlation between magnesium (Mg) intake and bone mineral density (BMD), and between the rate of bone loss and low Mg intake (Yano et al., 1985; Freudenheim et al., 1986; Angus and Sambrook, 1988; Tucker et al., 1999). In addition, there is strong evidence that Mg insufficiency is a risk factor for bone frailty when associated with ageing and menopause (Cohen and Kitzes, 1981; Rude, 1998; Stendig-Lindberg et al., 1993; Sojka and Weaver, 1995). Mg is the fourth most abundant cation in the human body (Maguire and Cowan, 2003; Wolf and Cittadini, 2003), with more than fifty percent of its total content stored in bone (Wallach, 1990). Mineral crystals in bone consist of mainly calcium phosphates, such as hydroxyapatite, which often show substitution of its calcium (Ca) ions by Mg^{2+}, CO_3^{2-}, Na^-, Sr^{2+} and HPO_4^2, among other ionic particles. Yet the influence of Mg on the mechanical and ultrastructural properties of mineralized bone matrix is often overlooked.

Osteocalcin and matrix Gla protein, non-collagenous constituents of the bone extracellular matrix, are known for containing γ-carboxyglutamic acid and for binding to mineral crystals (Hauschika et al., 1975; Price et al.,

1976). Non-carboxylated human osteocalcin possesses three glutamate residues at the positions 17, 21 and 24 of its amino acidic chain (Cairns and Price, 1994). Post-transcriptional maturation in the presence of vitamin K permits γ-carboxylation of osteocalcin, enabling further binding to the Ca ions of hydroxyapatite [$Ca_{10}(PO_4)_6(OH)_2$] (Price and Nishimoto 1980; Hauschka and Carr, 1982; Price and Williamson 1985). Recently, the discovery of the crystal structure of porcine osteocalcin by X-ray analysis has revealed a negatively charged protein surface with three Gla residues in helix 1, as well as conserved Aps residues in helix 2, a surface that would complement Ca ions in a hydroxyapatite crystal lattice (Hoang et al., 2003). Binding between osteocalcin and Ca may be related with the mechanisms that guide the ultrastructural alignment of mineral crystals in bone. However, vitamin K-dependent bone Gla protein is incompletely γ-carboxylated in a physiological state (Cairns and Price, 1994). Supported by this background, a vitamin K2 compound, MK-4 (menatetrenone), has been used as an alternative treatment for osteoporosis by putatively promoting γ-carboxylation of Gla-proteins. Yet the precise role of Gla proteins in bone mineral crystals is incompletely understood.

Kobayashi and his group have found that Mg-insufficient rats developed bones that are fragile under mechanical loading, despite high BMD values (2004). Interestingly, MK-4 administration improved bone strength parameters, such as maximum load and elastic modulus on Mg-insufficient bones, from which one may infer that MK-4 increased bone quality. Bone quality is presently a highlighted term related to osteoporosis prevention, treatment, and bone regeneration, and a recent concept established at the NIH consensus meeting suggests that bone strength depends on many factors, including mineralization, architecture, turnover, and presence of organic proteins in bone (NIH Consensus Development Panel on Osteoporosis Prevention, Diagnosis and Therapy. 2001).

Ultrastructural alterations of bone matrix that may relate to bone quality, such as those provoked by Mg insufficiency or vitamin K2 supplementation, are worthy of careful, serious study. By employing morphological analysis – immunohistochemistry, bone histomophometry, ultrastructures of mineralization and collagen fibrils, elemental mapping of Mg, Ca and phosphorus (P), and X-ray diffraction for mineral crystals – we attempted to elucidate the ultrastructural and elemental aspects of bone mineralization in Mg-insufficient bone with and without supplementation with vitamin K2.

Materials and methods

Animals and tissue preparation for histological examinations

Forty-five 4-week-old Wistar male rats (CLEA Japan, Inc., Tokyo) were randomly divided in 3 groups and fed with 1) a normal diet (control group: 0.09% Mg, 0.5% Ca, 0.66% Pi; CLEA Japan, n=15), 2) a Mg-insufficient diet (low Mg group: 0.006% Mg, 0.5% Ca, 0.66 % Pi; n=15), or 3) a Mg-insufficient diet supplemented by MK-4 (MK-4 group: 30mg MK-4/100g, Eisai, Co., Ltd., Tokyo, Japan, 0.006% Mg, 0.5% Ca, 0.66 % Pi; n=15) during 4 weeks, as previously described by Kobayashi et al. (2004). As described above, the mean dose of MK-4 during this experiment was 30 mg/kg of body weight, calculated from the food intake, MK-4 content of the diet (28 mg/100g food), and body weight. In all three groups, food intake was restricted to 80% of the average consumed by Wistar rats of the same age. Animals had access to distilled water *ad libitum*, and were maintained in a controlled environment set to 23±2°C and 55±15% humidity with a 12 h light–dark cycle. All animal procedures were in accordance with the Guidelines for Animal Experimentation of Niigata University. For bone labeling, calcein (10 mg/kg, Dojindo Laboratories, Kumamoto, Mashikimachi, Japan) was injected 12 and 5 days before sacrifice. Anesthesia was performed with diethyl ether and pentobarbital (Nembutal, Dinabot, Osaka, Japan), and perfusion proceeded with either 4% paraformaldehyde in 0.1 M cacodylate buffer (pH 7.4) or with a mixture of 2% paraformaldehyde and 2.5% glutaraldehyde in 0.067 M cacodylate buffer injected through the cardiac left ventricle. Femora and tibiae were removed and immersed in the same fixative for 12 h at 4°C. Some specimens were then demineralized with 5% EDTA solution and dehydrated with increasing concentrations of ethanol before paraffin embedding. Additionally, specimens destined for transmission electron microscope (TEM) observations were post-fixed with 1% OsO_4 in 0.1 M cacodylate buffer (pH 7.4) for 4 h at 4°C, dehydrated with ascending concentrations of acetone and embedded in epoxy resin (Taab, Berkshire, UK). Ultra-thin sections from these blocks were obtained with a microtome (Leica, Wein, Austria) and stained with tannic acid, uranyl acetate, and lead citrate for TEM examination (Hitachi H-7000 Hitachi Co. Ltd, Tokyo, Japan) at 80 kV. Mineralized bone matrix was also observed under TEM, with non-decalcified tibial and femoral specimens being post-fixed with 1% OsO_4 in 0.1 M cacodylate buffer (pH 7.4) for 4 h at 4°C prior to epoxy resin-embedding. One hundred nm-thick sections of these specimens were obtained with the use of ethylene glycol.

Immunohistochemistry

Dewaxed paraffin sections were examined for alkaline phosphatase (ALPase) reactivity as previously reported (Amizuka et al., 1999). Concisely, sections were immersed in 0.3% H_2O_2 in methanol for 30 min to block endogenous peroxidase. For reducing non-specific binding, 1% bovine serum albumin (Serologicals Proteins Inc. Kankakee, IL) in PBS (1%BSA-PBS) was applied on the sections for 20 min. Sections were then

incubated with a rabbit polyclonal antiserum against ALPase (Oda et al., 1999) at a dilution of 1:200 with 1% BSA-PBS at room temperature for 2 h and, after several washings in PBS, further incubated with horseradish peroxidase-conjugated anti-rabbit IgG (Chemicon International Inc., Temecula, CA) for 1 h. For visualization, diaminobenzidine tetrahydrochloride (DAB) was employed as substrate. For tartrate-resistant acid phosphatase (TRAPase) detection (Amizuka et al., 1998), sections were incubated in a mixture of 8 mg of naphthol AS-BI phosphate (Sigma, St. Louis, MO, USA), 70 mg of red violet LB salt (Sigma) and 50 mM L(+) tartaric acid (0.76 g, Nacalai Tesque, Kyoto, Japan) diluted in 60 ml of a 0.1M sodium acetate buffer (pH 5.0) for 20 min at 37°C. Methyl green was employed for counterstaining all sections.

Assessment by X-ray diffraction

Specimens from control, low Mg and MK-4 groups were sintered at 700°C for 4 h. The sintered material was crushed into smaller particles for X-ray diffraction analysis (JDX-3532, JEOL Ltd, Japan) at 40 KV and 30 mA acceleration at a scanning rate of 2°/min, with a sampling interval of 0.02°, and with a scanning range (2θ) of 10° to 80°. Counts were collected at goniometer for 0.5 seconds at each step. All data were analyzed with suitable software (MDI JADE6 software, XRD pattern processing, Material Data, Inc.).

Area analysis of Ca, P and Mg mapping by electron probing microanalyzer (EPMA)

After perfusion, tibial specimens were immersed in 70% ethanol and then dehydrated with ascending concentrations of methanol prior to epoxy resin embedding (Epoxicure resin, Buehler, Germany). Specimens were cut in the central region parallel to their longitudinal axis, then polished and carbon-coated (JEE-420; JEOL) to prevent charging prior to EPMA examination (JXA-8200; JEOL). The data were represented by area analysis. Cortical bone areas were measured using a beam current of 40 mA and an accelerating voltage of 15 kV (Hosoya et al., 2005).

Quantitative analyses of bone histomorphometry

Tibiae of control, low Mg and MK-4 groups (n=7 each) were removed and immersed in 70% ethanol prior to embedding in methyl methacrylate. The metaphyseal area of the longitudinal section encompassing the growth plate cartilage until an imaginary transverse line 1.5 mm proximal to the growth plate was employed for bone histomorphometry as described previously (Asawa et al., 2004a). The cortical bones were not included in the sampling area, which was examined under fluorescent microscopy (BX-50, Olympus Co. Ltd. Tokyo) to evaluate BV/TV (bone volume/tissue volume), Tb/Th (trabecular thickness), ES/BS (erosion surface/bone surface), BRs.R (bone resorption rate), N.Oc/BS (the number of osteoclasts/bone surface), Oc.S/BS (the osteoclast surface/bone surface), Ob.S/BS (the osteoblast surface/bone surface), OV/OS (osteoid volume/osteoid surface), MAR (mineral appositional rate) and MS/BS (mineralization surface/bone surface). Statistical analysis was performed by Student's t-test. All data were expressed as the mean + standard error of the mean (SEM).

Results

Magnesium (Mg)-insufficiency enhances osteoclastic activity, but administration of MK-4 inhibits it

In their tibial metaphyses, rats fed with Mg-insufficient diet (low Mg group) showed trabeculae shorter than those of the control group (Fig. 1). However, rats fed with a low Mg diet supplemented with MK-4 (MK-4 group) displayed relatively longer metaphyseal trabeculae, although not reaching the length found in control specimens. Immunohistochemistry for ALPase, a hallmark of osteoblastic cells, showed intense immunopositive osteoblastic cell layers for all three groups (Fig.1G-I). When examined under higher resolution, however, both low Mg and MK-4 groups showed a thicker osteoid layer compared to the control group (Fig.1J-L). In contrast, TRAPase-positive osteoclasts accumulated at the termini of tibial trabeculae of low Mg and MK-4 groups (Fig. 2A-C). Both groups showed many neighbouring osteoclasts on their metaphyseal bone surfaces (Fig. 2D-F). TEM observations showed well-developed ruffled borders on osteoclasts from the low Mg group, while osteoclasts in the MK-4 group often showed impaired ruffled borders (Fig. 2G-L).

Therefore, the recovery of bone strength in the MK-4 group (Kobayashi et al., 2004), may be, at least in part, due to a MK-4-induced inhibition of the accelerated osteoclastic activity provoked by Mg insufficiency.

Mg insufficiency causes structural alterations and an increment of the Ca content of bone mineral crystals

Once high values for BMD in the Mg-insufficient bone were reported (Kobayashi et al., 2004) and histological analysis alone could not provide a reasonable explanation for that fact, we further examined the ultrastructure of the mineralized bone matrix. When observed under TEM, mineral crystals in Mg-deficient bones were larger than those found in the control and MK-4 groups (Fig. 3A-C). Electron diffraction analysis of the mineralized bone matrix has shown similar number, intensity and diameters of electron rings for all three groups, suggesting that their crystal lattices are nearly the same (Fig. 3D-F). However, due to a low Mg diet, the bone matrix may have been affected in its constitution, likely showing a reduced content of Mg and altered ratios of other minerals. We have, therefore,

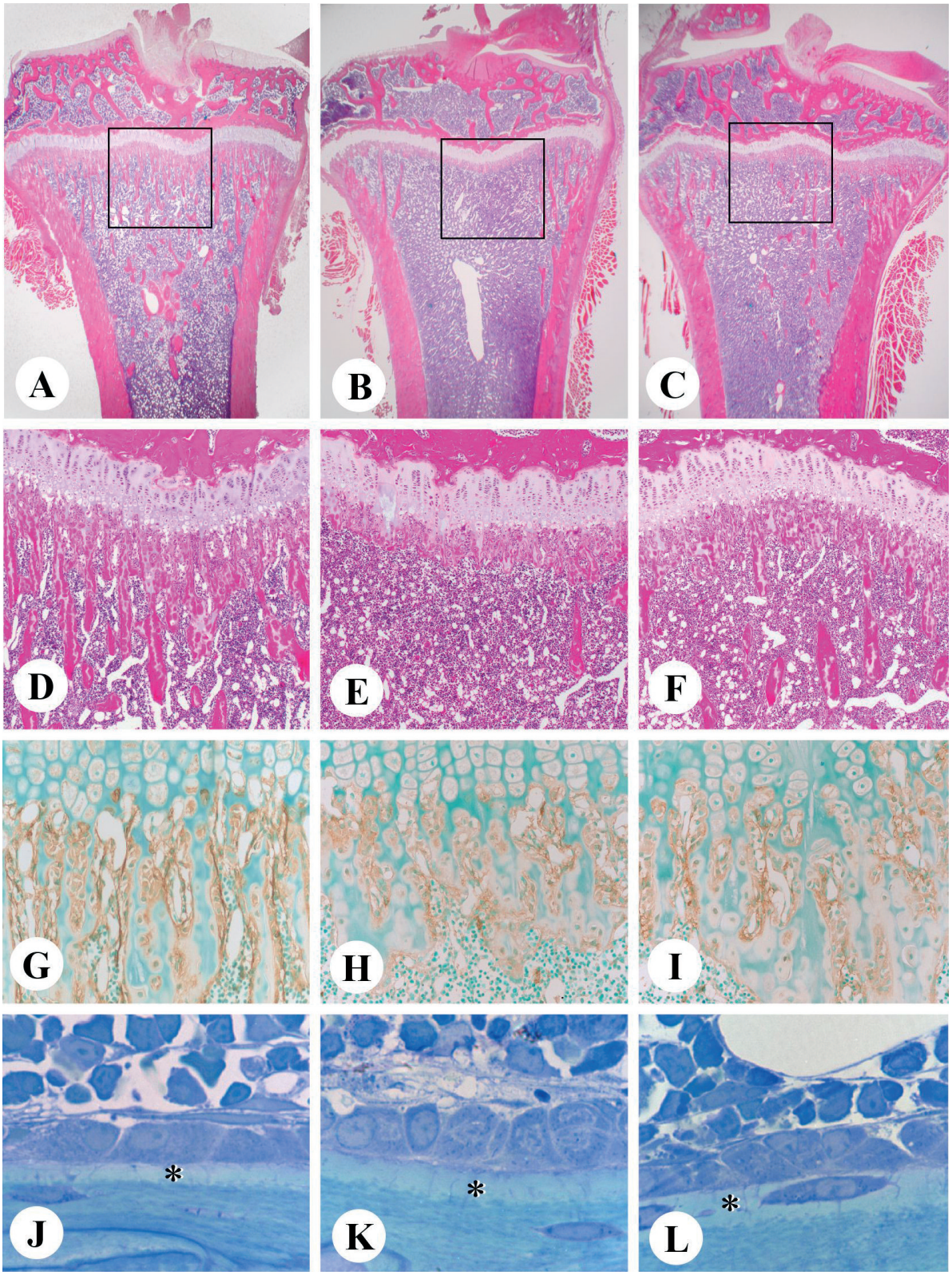

Fig. 1. Histological alterations in low Mg and MK-4 groups. Panels **D, E and F** are magnified views of the squares in panels **A, B and C**. Low Mg group **(B, E)** features shorter metaphyseal trabeculae than those of control group **(A, D)**. MK-4 group **(C, F)** displays relatively elongated metaphyseal trabeculae. No difference in the thickness of the growth plate exists among the three groups. Osteoblastic cell layers of control **(G)**, low Mg **(H)** and MK-4 **(I)** groups show similar ALPase immunoreaction. Under higher magnification, semi-thin sections reveal that both low Mg **(K)** and MK-4 **(L)** groups had a thicker osteoid layer (asterisks) under cuboidal osteoblasts when compared to control group **(J)**. A-C, x 10; D-F x 50; G-I, x 200; J-L, x 800

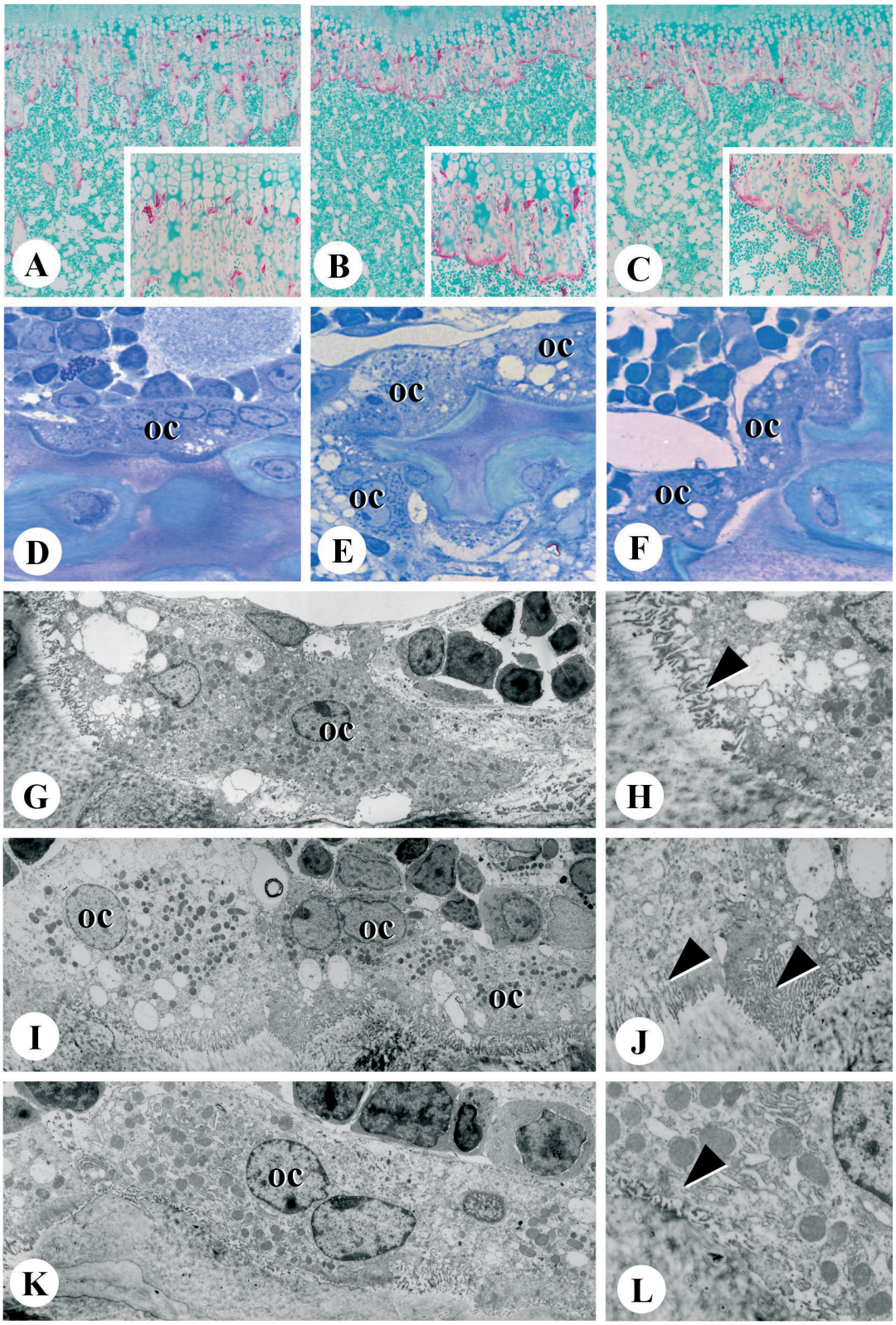

Fig. 2. Osteoclasts in control, low Mg and MK-4 groups. TRAPase-positive osteoclasts accumulate at the termini of the tibial trabeculae in both low Mg **(B)** and MK-4 groups **(C)**, while control bone shows scattered TRApase-positive osteoclasts **(A)**. Insets are amplified views of metaphyseal trabeculae. Semi-thin sections from epoxy resin-embedded specimens show neighboring osteoclasts (oc) in low Mg **(E)** and MK-4 **(F)** groups, but not in control **(D)**. Under TEM, low Mg group osteoclasts (oc) feature more exuberant ruffled borders **(I, J)** than control osteoclasts **(G, H)**. In MK-4 group **(K, L)**, osteoclasts possess poorly-developed ruffled borders, but still they accumulated on metaphyseal bone. Note underdeveloped ruffled borders on MK-4-treated osteoclasts (L) compared with those from low Mg osteoclasts (J). A-C, x50; D-F, x800; G, I, K; x2000, H, J, L; x4000

examined Ca, P and Mg mappings through an EPMA area analysis. Mg concentration was markedly decreased in the metaphyses and diaphyses of both low Mg and MK-4 groups, while the concentration of Ca, another bivalent cation, was dynamically increased (Fig. 4). P concentrations did not change among the groups. The altered concentrations of Ca and Mg may have affected the chemical formulae of apatite crystals of low Mg and MK-4 bones. Through X-ray diffraction analysis, peak patterns of control samples were shown to differ from either native or a pure form (synthetic) of hydroxyapatite, indicating the variety of mineral crystals existent in a normal bone (Fig. 5A). Alternatively, both low Mg and MK-4 samples showed peak patterns resembling those of a synthetic hydroxyapatite (Fig. 5B,C).

Premature mineralization of collagen fibrils induced by Mg-insufficiency is hindered by MK-4

In the osteoid of control group, mineralized nodules contacted with surrounding collagen fibrils, and appositional collagen mineralization appeared to expand along their longitudinal axis starting from the contact point (Fig. 6A). In the Mg-insufficient micro-environment, however, collagen fibrils often showed a different pattern of mineralization, which occurred uniformly and directly along the fibrils and featured no association with mineralized nodules (Fig. 6B). Alternatively, with MK-4 supplementation, this direct mineralization was markedly diminished and instead, again associated with mineralized nodules (Fig. 6C). The osteoid of low Mg bones featured collagen fibrils that were broken into fine filamentous structures. These filamentous regions of the collagen related to points of direct and premature mineralization (Fig. 7A-C). In the MK-4 group, in contrast, collagen fibrils showed the rigid structure characteristic of collagen fibrils, like control bone (Compare Figs. 6A and 7F-H). In the deepest portions of its bone matrix, Mg-deficient bone had filamentous fragments of collagen fibrils, as detected also in its osteoid (Fig. 7D, E). MK-4 bones, on the other hand, displayed rigid collagen fibrils showing unaltered configuration and striations (Figs. 7I, J).

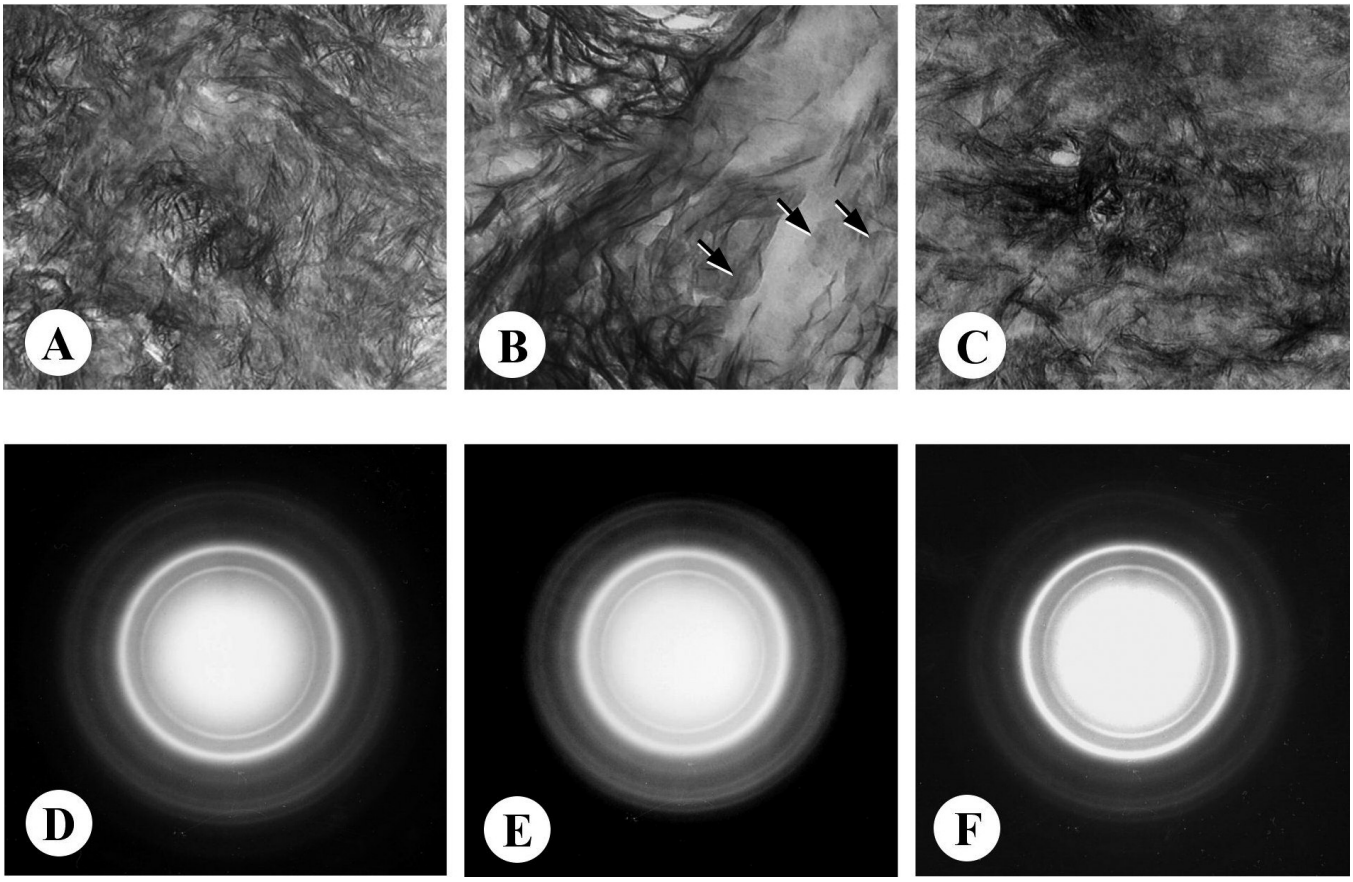

Fig. 3. TEM images of mineral crystals and electron diffraction. Mineral crystals (arrows) in low Mg bone **(B)** are larger than those of control **(A)** and MK-4 **(C)** group, both showing plate-like or ribbon-like mineral crystals. Electron diffraction demonstrates similar number, intensity and electron rings diameters for all groups **(D, E, F)**. A-C, x 100,000

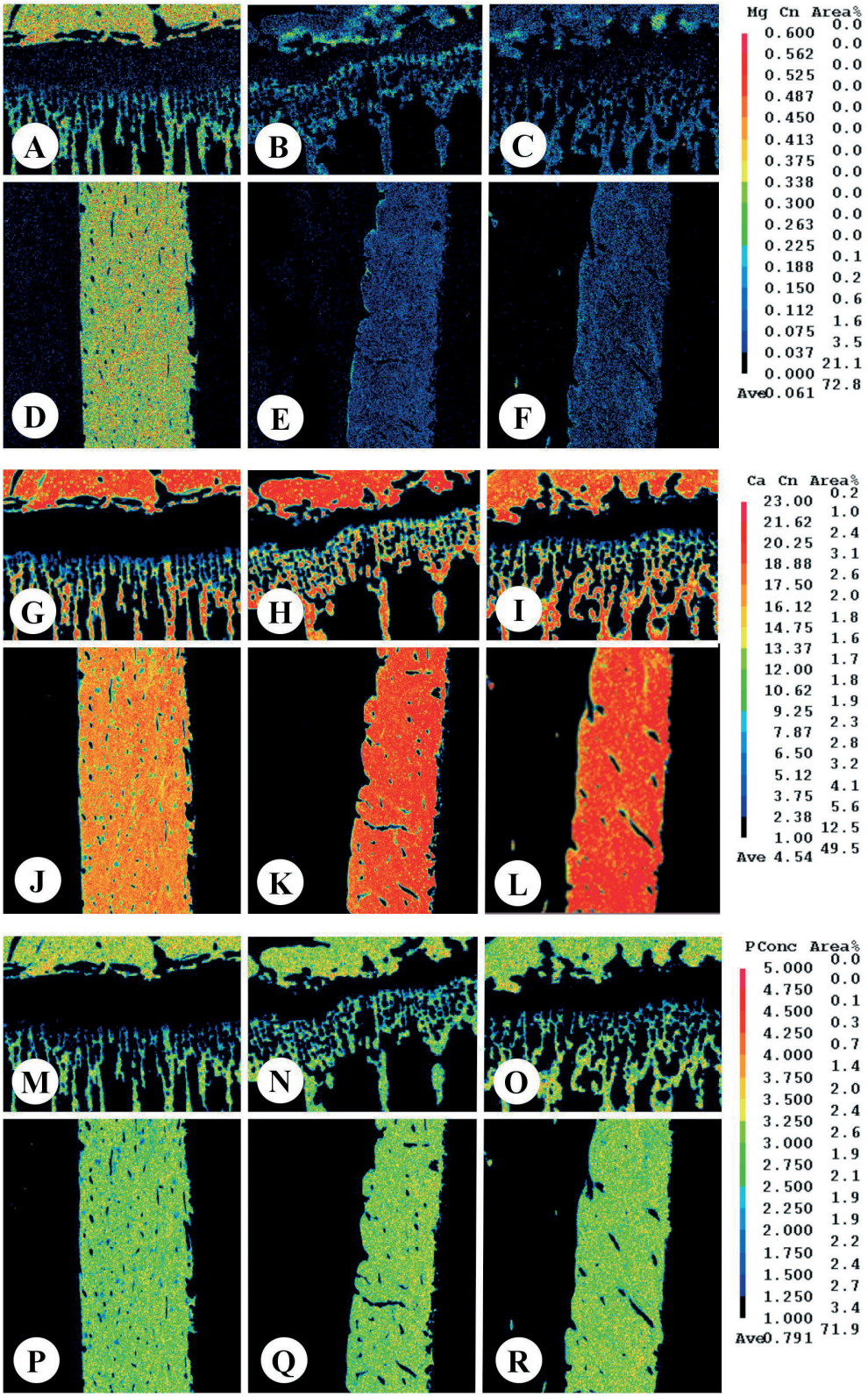

Fig. 4. Elemental mapping of Mg, Ca and P. In the analysis of elemental concentration, a visual color scale changing from dark blue to red as the concentrations increase. Compared with control (**A, D,** greenish yellow), the concentration of Mg in both low Mg (**B, E,** dark blue) and MK-4 groups (**C, F,** dark blue) is diminished. Ca concentration markedly increases in low Mg (**H, K,** red) and MK-4 (**I, L,** red) groups compared with control bone samples (light orange color, **G, H**). Note no difference in Ca concentrations (red color) between low Mg and MK-4 groups. Unlike Ca and Mg concentrations, that of P is similar among control (**M, P**), low Mg (**N, Q**) and MK-4 (**O, R**) groups (greenish yellow). x 40

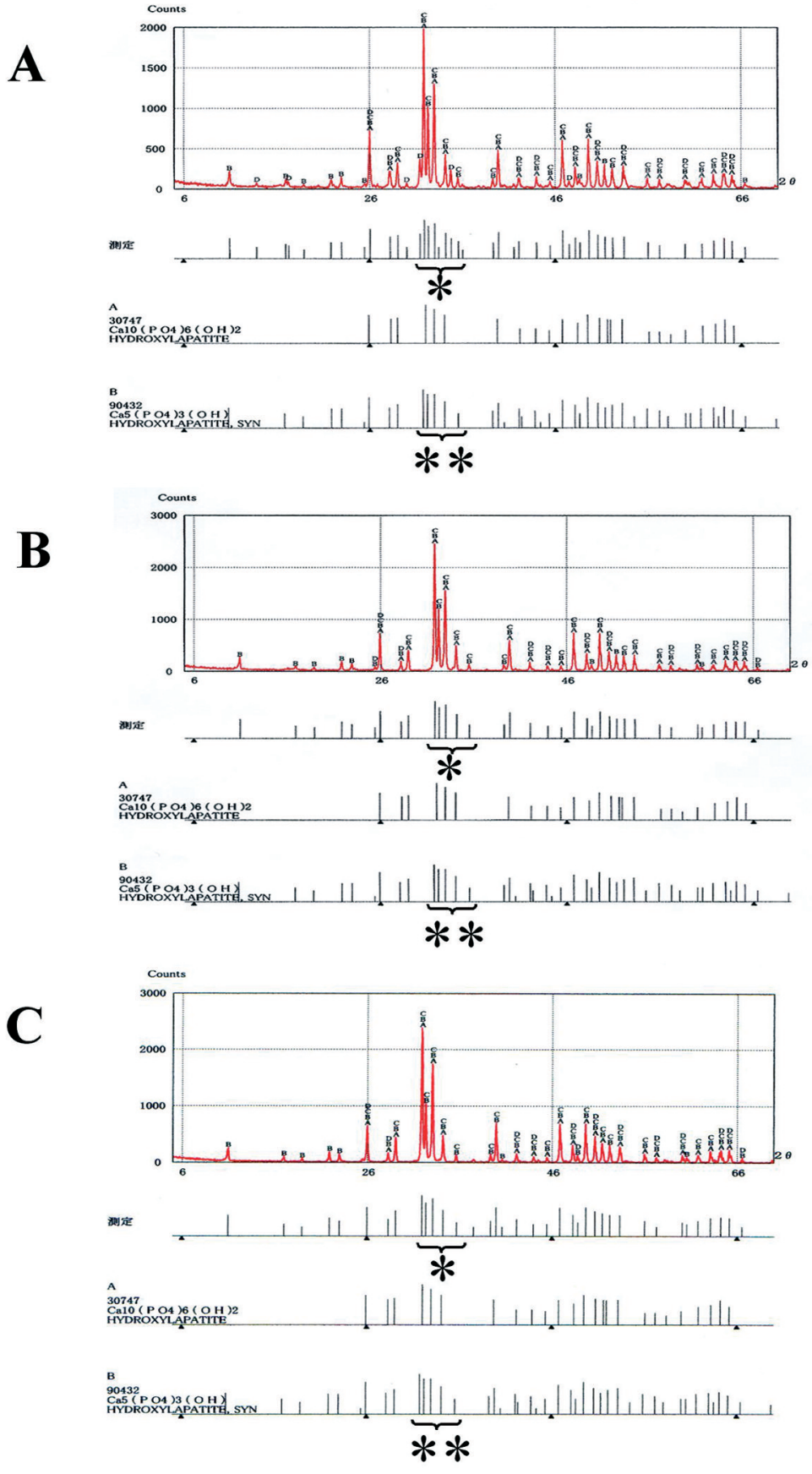

Fig. 5. Peak patterns of X-ray diffraction analysis. Upper graphics in **A** (control), **B** (low Mg) and **C** (MK-4) show the peak patterns of diffracted X-ray at goniometer (θ=66), running step-scan at 40 kV and 30 mA. The vertical axis records X-ray intensity, while the horizontal axis indicates angles in degrees 2θ. The lower panels are simplified images of the graphics. Control peak patterns of high counts (single asterisk, A) are not similar to either native $[Ca_{10}(PO_4)_6(OH)_2]$ or to a pure (synthetic) form of hydroxyapatite $[Ca_5(PO_4)_3(OH)]$. Compare the patterns indicated by single and double asterisks. In contrast, low Mg **(B)** and MK-4 **(C)** samples show patterns (single asterisks) similar to those of synthetic hydroxyapatite (double asterisks).

Statistical analyses of bone histomorphometry reflecting bone mineralization

In order to ratify our histological and ultrastructural findings, we examined parameters such as BV/TV, Tb/Th, ES/BS, N.Oc/BS, Oc.S/BS, Ob.S/BS, BRs.R and OV/OS to assess static parameters, and MAR and MS/BS for a picture of bone dynamics (Fig.8). The parameters of BV/TV, Tb/Th, ES/BS, N.Oc/BS, Oc.S/BS, Ob.S/BS indicated increased osteoclastic number and activity, resulting in reduced bone volume in the low Mg group with a slight recovery of bone volume in the presence of MK-4. Although not statistically significant, these values confirmed our histological

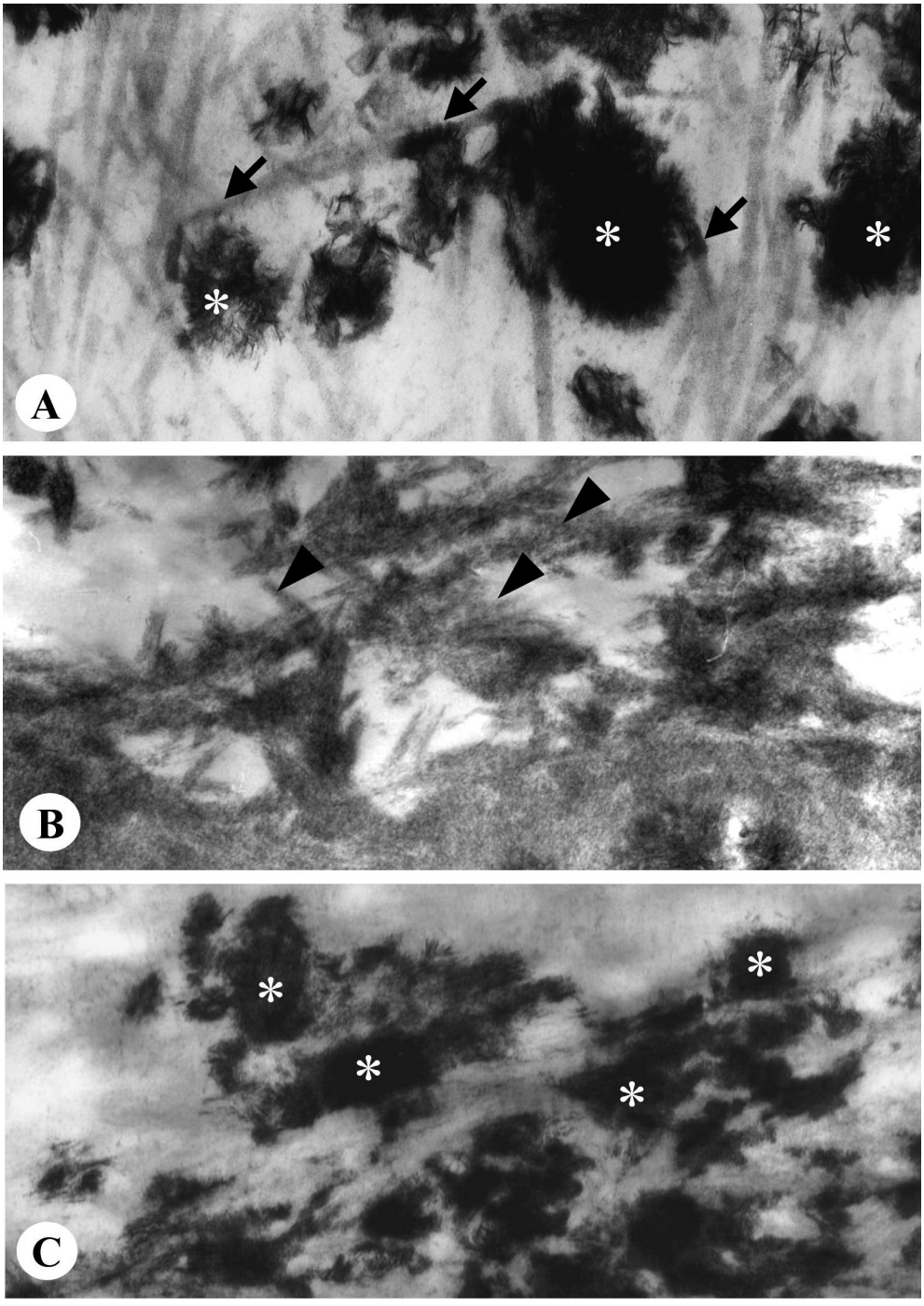

Fig. 6. Ultrastructures of collagen mineralization in the osteoid layer. In the osteoid of control bones **(A)**, mineralized nodules (asterisks) associate with surrounding collagen fibrils. Note contact points (arrows) between mineralized nodules and collagen fibrils. However, in low Mg bone **(B)**, collagen fibrils mineralize without associating to mineralized nodules. Strong black color indicates mineralization, and the straight corpuscles represent collagen fibrils (arrowheads). Few mineralized nodules are present. When supplemented with MK-4 **(C)**, collagen mineralization again associates with mineralized nodules (asterisks). x 30,000

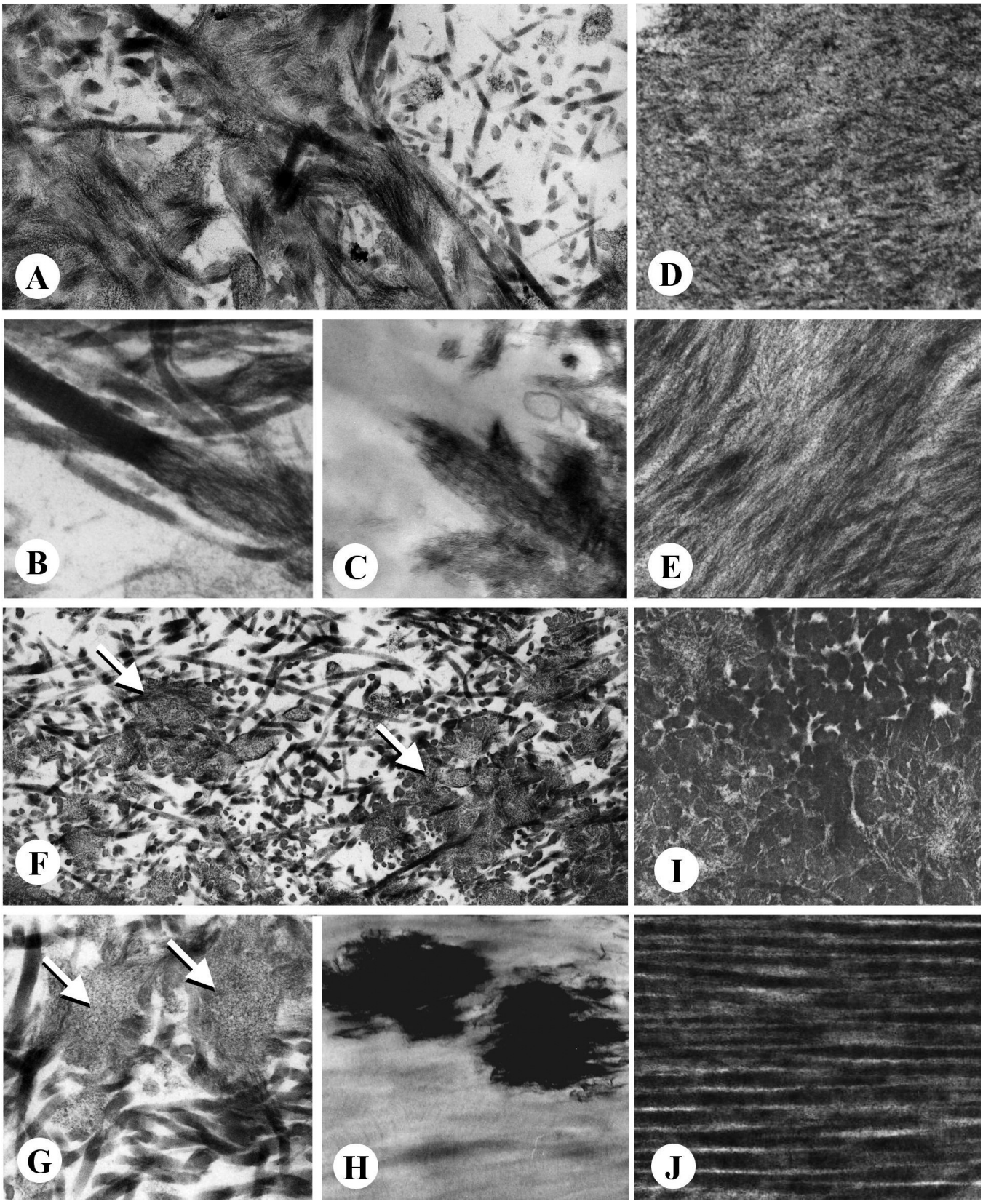

Fig. 7. Direct mineralization of collagen fibrils and filamentous fibrillar structures in low Mg group. When collagen fibrils are submitted to electron staining with tannic acid, uranyl acetate and lead citrate, they feature a woven-like appearance **(A)**. Collagen fibrils **(B)** are shown to collapse into fine filamentous structures indicating direct mineralization **(C).** In its deepest portions, Mg-deficient bone displays filamentous structures in both cross **(D)** and longitudinal sections **(E)**. Collagen fibrils of MK-4 group share their space with spherical dark areas compatible with mineralized nodules (arrows, **F**). At a higher magnification, these amorphous structures (arrows) associate with collagen fibrils (**G)**. When undemineralized samples of the same group are examined, spherical mineralized nodules identical to those structures in panel G are seen among the collagen fibrils **(H)**. In the deepest portions of MK-4 group specimens, collagen fibrils maintain their rigid structures featuring proper configuration **(I)** and striations **(J)** in the cross and longitudinal sections, respectively. A, F, x 15,000; B-E, x 30,000; G-J, x 30,000

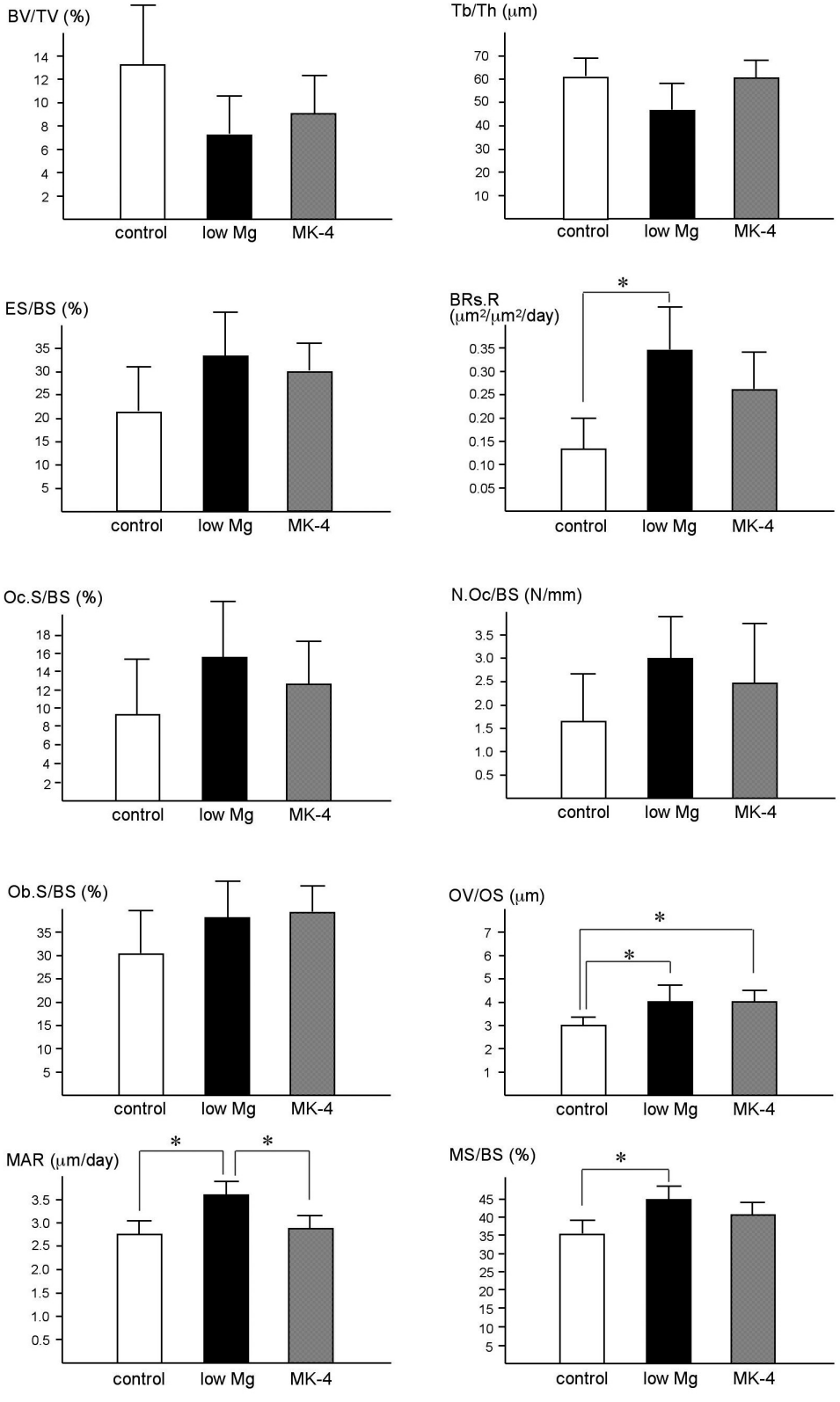

Fig. 8. Statistical analysis on the parameters of bone histomorphometry BV/TV (%), Tb/Th (μm), ES/BS (%), BRs.R ($\mu m^2/\mu m^2$/day), Oc.S/BS (%), N.Oc/BS (N/mm), Ob.S/BS (%), OV/OS (μm), MAR (μm/day), MS/BS (%) were examined in the metaphyseal area of the control, low Mg and MK-4 groups (See Materials and Methods). Statistical analysis was performed by Student's t-test. All data was expressed the mean ± SEM.

findings. An increased BRs.R indicated accelerated osteoclastic resorption in the low Mg group. The OV/OS showed a significant increase of the osteoid layer in both the low Mg and MK-4 groups, which are consistent with the findings in Figs.1J-1L. Therefore, bone turnover may be accelerated when Mg is not included in the diet. Noteworthy are the data on MAR and MS/BS: these parameters were significantly increased in the low Mg groups compared with control ones. With MK-4, the values for these parameters were reduced, and were statistically significant for MAR.

Discussion

Combined accelerated osteoclastic resorption and abnormal mineralization of collagen fibrils may reduce the strength of Mg-deficient bones. Even though vitamin K2, *i.e.*, MK-4, has already been reported to inhibit osteoclastic activities (Hara et al., 1994; Akiyama et al., 1994, 1999; Koshihara et al., 2003; Asawa et al., 2004a; Nanke et al., 2005), our work is the first to demonstrate that it can rescue the abnormal collagen mineralization caused by Mg-insufficiency. MK-4 seems to enhance bone properties through two distinct mechanisms: first, by inhibiting osteoclastic bone resorption, and second, by normalizing collagen mineralization.

Osteoblasts in the three groups were cuboidal in shape and displayed similar ALPase intensity, suggesting an unaltered osteoblastic activity that would not explain the undersized trabeculae found on the low Mg group. In agreement with Rude et al. (2003, 2004), and as shown in Figs. 2 and 8, we have observed that Mg-deficiency stimulated osteoclastic activity. MK-4 inhibited resorption in our experiments as previously reported (Akiyama et al., 1994, 1999; Hara et al., 1994; Koshihara et al., 2003; Asawa et al., 2004a; Nanke et al., 2005). Based on our data, it seems that the recovery of bone strength in the MK-4 group might be, at least in part, due to inhibition of over-accelerated osteoclastic activities. In other words, Mg-deficiency may accelerate osteoclastic bone resorption, which on the other hand could be brought back to acceptable levels by MK-4 administration.

As reported by Kobayashi et al. (2004), the increase in BMD values in the low Mg group is still a puzzling issue, which prompted us to examine the ultrastructural properties of the mineralized bone matrix in that group. We demonstrated that a Mg-insufficient diet not only diminishes Mg content in bone, but also elevates Ca concentrations, provoking an abundance of pure hydroxyapatite. Furthermore, Mg-insufficiency caused direct mineralization of collagen fibrils, which collapsed into fine filamentous structures. Although MK-4 did not influence Ca and Mg concentrations or the chemical formulae of apatite crystals, it hindered the early mineralization of collagen fibrils, by recovering their association with mineralized nodules. In addition, bone histomorphometry data showed increased MAR (mineral appositional rate) and MS/BS (ratio of mineralizing surface) in the low-Mg bone, while MK-4 supplementation was shown to normalize the speed of mineralization (Fig. 8). Therefore, the increased values for MAR and MS/BS in the low Mg bone may reflect the direct mineralization of collagen fibrils, without the mediation by mineralized nodules seen in healthy bones. Bone mineral crystals may be affected by the availability and concentrations of mineral elements that compose their lattices; the processes of collagen mineralization associated with mineralized nodules, however, seem to be determined by other variables, *e.g.*, vitamin K-dependent non-collagenous Gla proteins.

Surrounding bone mineral crystals there is a hydrogen layer that establishes a state of dynamic equilibrium of mineral elements. As Mg can substitute Ca in apatite crystals (Aoba et al., 1992), we postulate that a low Mg diet reduces the absolute number of Mg ions in the hydrogen layer, which reduces the Mg content in the crystal lattice. In this context, the content of Ca increases as a compensation for the Mg-insufficiency. Ca bivalent cations would then occupy available positions in the crystal net created by Mg-deficiency, reestablishing a pure hydroxyapatite crystal configuration. Mg is also known as a disruptor of crystal growth (Blumenthal et al., 1977; Bigi et al., 1992; Sojka and Weaver 1995). Mg-insufficiency was consistently shown to enlarge mineral crystals (Fig. 3A-C). We have raised the conjecture that an increased concentration of Ca and the existence of a purer and overgrown form of apatite crystals would explain the high BMD values in Mg-insufficient bones (Kobayashi et al., 2004). Excessive growth and pureness of apatite crystals, however, do not seem to translate into bone strength, and apparently worsen it, instead (Boskey et al., 2003).

The initial process of bone mineralization in a physiological state is mediated by matrix vesicles (Yamada and Ozawa, 1978; Anderson et al., 1975; Anderson, 1995, 2003), which grow into mineralized nodules and subsequently enable appositional mineralization of collagen fibrils (Takano et al., 2000; Hoshi et al., 2001a; Asawa et al., 2004b). During this process, mineral crystals derived from mineralized nodules may arrange themselves properly into the collagen fibrils (Nakano et al., 2002). In contrast, a Mg-insufficient micro-environment would facilitate nucleation of apatite crystals, since Mg is an inhibitor of apatite nucleation (Blumenthal et al., 1977; Bigi et al., 1992; Sojka and Weaver, 1995). Additionally, increased concentrations of Ca may ease binding with the abundantly preexisting phosphates (Hoshi et al., 2001a), resulting in mineral crystal aggregates that act as nuclei for collagen mineralization. Although neither mineral composition nor chemical formulae of apatite crystals were affected (Figs. 4, 5), MK-4 supplementation did normalize collagen mineralization (Fig. 6). MK-4 enhances γ-carboxylation of osteocalcin, which was shown to inhibit nucleation of apatite crystals (Hunter et al., 1996). Mg is a potent inhibitor of osteocalcin binding to hydroxyapatite (Wians et al., 1990) and, therefore,

decreased Mg may foster apatite crystal nucleation. MK-4 supplementation may enhance γ-carboxylation of osteocalcin, hindering Mg-deficiency-driven direct mineralization of collagen fibrils; on the other hand, enhanced γ-carboxylation of Gla protein by MK-4 may increase mineral crystal binding (Hoang et al., 2003), easing the development of mineralized nodules.

Mineralized nodules, which derive from matrix vesicles (Anderson et al., 1975; Anderson, 1995, 2003), may act as regulators of collagen mineralization. Organic components surround the crystals of mineralized nodules, forming the so-called crystal sheath or crystal ghost (Hoshi et al., 2001b; Bonucci 2002), where osteocalcin makes a complex with osteopontin (Ritter et al., 1992). It is therefore likely that non-collagenous proteins serve to regulate the assembly and growth of mineral crystals. In normal mineralized nodules, vitamin K2-dependent γ-carboxylated osteocalcin seems to hamper the excessive crystalline nucleation (Hunter et al., 1996), while facilitating a correct mineral assembly that contributes to a normal mineralization of collagen fibrils. Without vitamin K2, we have observed mineral crystals to be spread all over the osteoid accompanied by few mineralized nodules, and have also demonstrated that mineral crystals were not aligned along the longitudinal axis of collagen fibrils (data not shown).

In summary, Mg-deficiency alters the elemental composition and chemical formulae of bone mineral crystals. The result is abnormal collagen mineralization, which can be rescued by vitamin K2 supplementation.

Acknowledgements: This work was partially supported by grants from the Salt Science Research Foundation (No. 0523, N Amizuka), and from the Japanese Society for the Promotion of Science (N Amizuka). The authors would like to thank Dr. Akemi Ito, Director, Ito Bone Histomorphometry Institute, for her invaluable assistance in bone histomorphometry

References

Akiyama Y., Hara K., Tajima T., Murota S. and Morita I. (1994). Effect of vitamin K2 (menatetrenone) on osteoclast-like cell formation in mouse bone marrow cultures. Eur. J. Pharmacol. 263, 181-185.

Akiyama Y., Hara K., Kobayashi M., Tomiuga T. and Nakamura T. (1999). Inhibitory effect of vitamin K2 (menatetrenone) on bone resorption in ovariectomized rats: a histomorphometric and dual energy X-ray absorptiometric study. Jpn. J. Pharmacol. 80, 67-74.

Amizuka N., Yamada M., Watanabe J.I., Hoshi K., Fukushi M., Oda K., Ikehara Y. and Ozawa H. (1998). Morphological examination of bone synthesis via direct administration of basic fibroblast growth factor into rat bone marrow. Microsc. Res. Tech. 41, 313-322.

Amizuka N., Kwan M.Y., Goltzman D., Ozawa H. and White J.H. (1999). Vitamin D3 differentially regulates parathyroid hormone/parathyroid hormone-related peptide receptor expression in bone and cartilage. J. Clin. Invest. 103, 373-381.

Anderson H.C. (1995). Molecular biology of matrix vesicles. Clin. Orthop. 314, 266-280.

Anderson H.C. (2003). Matrix vesicles and calcification. Curr. Rheumatol. Rep. 5, 222-226.

Anderson H.C., Cecil R. and Sajdera S.W. (1975). Calcification of rachitic rat cartilage in vitro by extracellular matrix vesicles. Am. J. Pathol. 79, 237-254.

Angus R.M. and Sambrook P.N. (1988). Dietary intake and bone mineral density. Bone Miner. 4, 265-277.

Aoba T., Moreno E.C. and Shimoda S. (1992). Competitive adsorption of magnesium and calcium ions onto synthetic and biological apatites. Calcif. Tissue Int. 51,143-150.

Asawa Y., Amizuka N., Hara K., Kobayashi M., Aita M., Li M., Kenmotsu S., Oda K., Akiyama Y. and Ozawa H. (2004a). Histochemical evaluation for the biological effect of menatetrenone on metaphyseal trabeculae of ovariectomized rats. Bone 35, 870-880.

Asawa Y., Aoki K., Ohya K., Ohshima H. and Takano Y. (2004b). Appearance of electron-dense segments: indication of possible conformational changes of pre-mineralizing collagen fibrils in the osteoid of rat bones. J. Electron Microsc. 53, 423-433.

Bigi A., Foresti E., Gregorini R., Ripamonti A., Roveri N. and Shah J.S. (1992). The role of magnesium on the structure of biological apatites. Calcif. Tissue Int. 50, 439-444.

Blumenthal N.C., Betts F. and Posner A.S. (1977). Stabilization of amorphous calcium phosphate by Mg and ATP. Calcif. Tissue Res. 23, 245-250.

Bonucci E. (2002). Crystal ghosts and biological mineralization: fancy spectres in an old castle, or neglected structures worthy of belief. J. Bone Miner. Metab. 20, 249-265.

Boskey A. (2003). Bone mineral crystal size Osteoporosis Int. 14, S16-S21.

Cairns J.R. and Price P.A. (1994). Direct demonstration that the vitamin K-dependent bone Gla protein is imcompletely γ-carboxylated in humans. J. Bone Miner. Res. 9, 1989-1997.

Cohen L. and Kitzes R. (1981) Infrared spectroscopy and magnesium content of bone mineral in osteoporotic women. Isr. J. Med. Sci. 17, 1123-1125.

Freudenheim J.L., Johnson N.E. and Smith E.L. (1986). Relationships between usual nutrient intake and bone-mineral content of women 35–65 years of age: Longitudinal and cross-sectional analysis. Am. J. Clin. Nutr. 44, 863-876.

Hara K., Akiyama Y., Nakamura T., Murota S. and Morita I. (1995). The inhibitory effect of vitamin K2 (menatetrenone) on bone resorption may be related to its side chain. Bone 16, 179-184.

Hauschika P.V., Lian J.B. and Gallop P.M. (1975). Direct identification of the calcium-binding amino acids, γ-calboxyglutamate, in mineralized tissue. Proc. Natl. Acad. Sci. USA. 72, 3925-3929.

Hauschka P.V. and Carr S.A. (1982). Calcium-dependent alpha-helical structure in osteocalcin. Biochemistry 21, 2538-2547.

Hoang Q.Q., Sicheri F., Howard A.J. and Yang D.S. (2003). Bone recognition mechanism of porcine osteocalcin from crystal structure. Nature 425, 977-980.

Hosoya A., Hoshi K., Sahara N., Ninomiya T., Akahane S., Kawamoto T. and Ozawa H. (2005). Effects of fixation and decalcification on the immunohistochemical localization of bone matrix proteins in fresh-frozen bone sections. Histochem. Cell Biol. 123, 639-646.

Hoshi K., Ejiri S. and Ozawa H. (2001a). Localizational alterations of calcium, phosphorus, and calcification-related organics such as proteoglycans and alkaline phosphatase during bone calcification. J. Bone Miner. Res. 16, 289-298.

Hoshi K., Ejiri S. and Ozawa H. (2001b). Organic components of crystal

sheaths in bones. J. Electron Microsc. 50, 33-40.

Hunter G.K., Hauschka P.V., Poole A.R., Rosenberg L.C. and Goldberg H.A.. (1996). Nucleation and inhibition of hydroxyapatite formation by mineralized tissue proteins. Biochem. J. 317, 59-64.

Kobayashi M., Hara K. and Akiyama Y. (2004). Effects of vitamin K2 (menatetrenone) and alendronate on bone mineral density and bone strength in rats fed a low-magnesium diet. Bone 35, 1136-1143.

Koshihara Y., Hoshi K., Okawara R., Ishibashi H. and Yamamoto S. (2003). Vitamin K stimulates osteoblastogenesis and inhibits osteoclastogenesis in human bone marrow cell culture. J. Endocrinol. 176, 339-348.

Maguire M.E. and Cowan J.A. (2002). Magnesium chemistry and biochemistry. Biometals 15, 203-210.

Nakano T., Kaibara K., Tabata Y., Nagata N., Enomoto S., Marukawa E. and Umakoshi Y. (2002). Unique alignment and texture of biological apatite crystallites in typical calcified tissues analyzed by microbeam X-ray diffractometer system. Bone 31, 479-487.

Nanke Y., Kotake S., Ninomiya T., Furuya T., Ozawa H. and Kamatani N. (2005). Geranylgeranylacetone inhibits formation and function of human osteoclasts and prevents bone loss in tail-suspended rats and ovariectomized rats. Calcif. Tissue Int. 77, 376-385.

NIH Consensus Development Panel on Osteoporosis Prevention, Diagnosis, and Therapy. (2001). Osteoporosis prevention, diagnosis, and therapy. JAMA. 285, 785-795.

Oda K., Amaya Y., Fukushi-Irie M., Kinameri Y., Ohsuye K., Kubota I., Fujimura S. and Kobayashi J. (1999). A general method for rapid purification of soluble versions of glycosylphosphatidylinositol-anchored proteins expressed in insect cells: an application for human tissue-nonspecific alkaline phosphatase. J. Biochem. 126, 694-699.

Price P.A., Otsuka A.S., Poser J.W., Kristaponis J. and Raman N. (1976). Characterizationn of a γ-carboxyglutamic acid containing protein from bone. Proc. Natl. Acad. Sci. USA 73, 1447-1451.

Price P.A. and Nishimoto S.K. (1980). Radioimmunoassay for the vitamin K-dependent protein of bone and its discovery in plasma. Proc. Natl. Acad. Sci. USA 77, 2234-2238.

Price P.A. and Williamson M.K. (1985). Primary structure of bovine matrix Gla protein, a new vitamin K-dependent bone protein. J. Biol. Chem. 260, 14971-14975.

Ritter N.M., Farach-Carson M.C. and Butler W.T. (1992). Evidence for the formation of a complex between osteopontin and osteocalcin. J. Bone Miner. Res. 7, 877-885.

Rude R.K. (1998). Magnesium deficiency: a heterogeneous cause of disease in humans. J. Bone Miner. Res. 13, 749-758.

Rude R.K., Gruber H.E., Wei L.Y., Frausto A. and Mills B.G. (2003). Magnesium deficiency: effect on bone and mineral metabolism in the mouse. Calcif. Tissue Int. 72, 32-41.

Rude R.K., Gruber H.E., Norton H.J., Wei L.Y., Frausto A. and Mills B.G. (2004). Bone loss induced by dietary magnesium reduction to 10% of the nutrient requirement in rats is associated with increased release of substance P and tumor necrosis factor-alpha. J. Nutr. 134, 79-85.

Sojka J.E. and Weaver C.M. (1995). Magnesium supplementation and osteoporosis. Nutr. Rev. 53, 71-74.

Stendig-Lindberg G., Tepper R. and Leichter I. (1993). Trabecular bone density in a two-year controlled trial of peroral magnesium in osteoporosis. Magnesium Res. 6, 155-163.

Takano Y., Sakai H., Baba O. and Terashima T. (2000). Differential involvement of matrix vesicles during the initial and appositional mineralization processes in bone, dentin, and cementum. Bone 26, 333-339.

Tucker K.L., Hannan M.T., Chen H., Cupples L.A., Wilson R.W.F. and Kiel D. (1999). Potassium, magnesium, and fruit and vegetable intakes are associated with greater bone mineral density in elderly men and women. Am. J. Clin. Nutr. 69, 727-736.

Wallach S. (1990). Effects of magnesium on skeletal metabolism. Magnes Trace Elem. 9, 1-14.

Wians F.H. Jr, Strickland D.M., Hankins G.D. and Snyder R.R. (1990). The effect of hypermagnesemia on serum levels of osteocalcin in an animal model. Magnes Trace Elem. 9, 28-35.

Wolf F.I. and Cittadini A. (2003). Chemistry and biochemistry of magnesium. Mol. Aspects Med. 24, 3-9.

Yamada M. and Ozawa H. (1978). Ultrastructural and cytochemical studies on the matrix vesicle calcification in the teeth of the killifish, Oryzias latipes. Arch. Histol. Jpn. 41, 309-323.

Yano K., Heilbrun L.K., Wasnich R.D., Hankin J.H. and Vogel J.M. (1985). The relationship between diet and bone mineral content of multiple skeletal sites in elderly women living in Hawaii. Am. J. Clin. Nutr. 42, 877-888.

Accepted June 6, 2008